Published OnlineFirst March 27, 2012; DOI:10.1158/1078-0432.CCR-11-1078

Table 2. Genes downregulated in cancer stroma, which are putative targets of miR-17-92a and/or miR-25-106b clusters (Cont'd)

Gene symbol	Genbank accession	Description	Fold Change[a]	Q (%)[a]	miR-17/20a/106b/93 target[b]	miR-18a target[b]	miR-19a/19b target[b]	miR-92a/25 target[b]
CCL13	NM_005408	*Homo sapiens* chemokine (C-C motif) ligand 13 (CCL13)	0.2404	1.2419				○
CCL5	NM_002985	*Homo sapiens* chemokine (C-C motif) ligand 5 (CCL5)	0.3839	1.2419	○	○	○	
IL9R	NM_176786	*Homo sapiens* interleukin 9 receptor (IL9R), transcript variant 2	0.4804	1.2419		○		
IL18R1	NM_003855	*Homo sapiens* interleukin 18 receptor 1 (IL18R1)	0.4667	1.2419			○	
IL29	NM_172140	*Homo sapiens* interleukin 29 (IFN, lambda 1; IL29)	0.4156	2.2195		○		
TNFRSF19	NM_018647	*Homo sapiens* TNF receptor superfamily, member 19 (TNFRSF19), transcript variant 1	0.4843	2.2195			○	
TSLP	NM_033035	*Homo sapiens* thymic stromal lymphopoietin (TSLP), transcript variant 1	0.3841	2.2195			○	
IL25	NM_022789	*Homo sapiens* interleukin 25 (IL25), transcript variant 1	0.4775	2.2195	○	○		
KEGG 04340 :Hedgehog signaling pathway								
WNT10A	NM_025216	*Homo sapiens* wingless type MMTV integration site family, member 10A (WNT10A)	0.1264	0.0000			○	
BMP2	NM_001200	*Homo sapiens* bone morphogenetic protein 2 (BMP2)	0.1734	0.0748	○	○		
BMP6	NM_001718	*Homo sapiens* bone morphogenetic protein 6 (BMP6)	0.2097	0.2025			○	
BMP5	NM_021073	*Homo sapiens* bone morphogenetic protein 5 (BMP5)	0.1747	0.3097				○
WNT9A	NM_003395	*Homo sapiens* wingless-type MMTV integration site family, member 9A (WNT9A)	0.3830	0.7799			○	
WNT1	NM_005430	*Homo sapiens* wingless-type MMTV integration site family, member 1 (WNT1)	0.4226	0.7799			○	
CSNK1A1	AF447582	*Homo sapiens* HLCDGP1 mRNA, complete cds.	0.4952	1.2419			○	
WNT7B	NM_058238	*Homo sapiens* wingless-type MMTV integration site family, member 7B (WNT7B)	0.4704	1.2419	○	○	○	
BMP8A	NM_181809	*Homo sapiens* bone morphogenetic protein 8a (BMP8A)	0.3596	2.2195				○
HHIP	AK074711	*Homo sapiens* cDNA FLJ90230 fis, clone NT2RM2000410	0.4494	3.4908				○
KEGG 05200 :Pathways in cancer								
CASP8	NM_033356	*Homo sapiens* caspase 8, apoptosis-related cysteine peptidase (CASP8), transcript variant C	0.1313	0.0000	○		○	
COL4A4	NM_000092	*Homo sapiens* collagen, type IV, alpha 4 (COL4A4)	0.0790	0.0000	○	○		
WNT10A	NM_025216	*Homo sapiens* wingless-type MMTV integration site family, member 10A (WNT10A)	0.1264	0.0000			○	
BCL2	NM_000633	*Homo sapiens* B-cell CLL/lymphoma 2 (BCL2), nuclear gene encoding mitochondrial protein, transcript variant α	0.2490	0.0353	○			○

(Continued on the following page)

Published OnlineFirst March 27, 2012; DOI:10.1158/1078-0432.CCR-11-1078

Table 2. Genes downregulated in cancer stroma, which are putative targets of miR-17-92a and/or miR-25-106b clusters (Cont'd)

Gene symbol	Genbank accession	Description	Fold Change[a]	Q (%)[a]	miR-17/20a/106b/93 target[b]	miR-18a target[b]	miR-19a/19b target[b]	miR-92a/25 target[b]
RASSF5	NM_182664	*Homo sapiens* Ras association (RalGDS/AF-6) domain family 5 (RASSF5), transcript variant 2	0.2031	0.0353			○	
BMP2	NM_001200	*Homo sapiens* bone morphogenetic protein 2 (BMP2)	0.1734	0.0748	○	○		
VHL	AF088066	*Homo sapiens* full-length insert cDNA clone ZD86C03.	0.3146	0.0748	○	○		
PDGFRA	BC015186	*Homo sapiens* platelet-derived growth factor receptor, α polypeptide, mRNA (cDNA clone IMAGE:4043984), complete cds	0.2247	0.1256	○			○
IGF1	NM_000618	*Homo sapiens* insulin-like growth factor 1 (somatomedin C; IGF1)	0.2991	0.2025		○	○	
ETS1	NM_005238	*Homo sapiens* v-ets erythroblastosis virus E26 oncogene homolog 1 (avian; ETS1)	0.3762	0.3097			○	○
TGFBR2	NM_003242	*Homo sapiens* TGF, β receptor II (70/80 kDa) (TGFBR2), transcript variant 2	0.3819	0.3097	○		○	
NKX3-1	NM_006167	*Homo sapiens* NK3 transcription factor related, locus 1 (*Drosophila*; NKX3-1)	0.4231	0.4833	○			
CBL	NM_005188	*Homo sapiens* Cas-Br-M (murine) ecotropic retroviral transforming sequence (CBL)	0.4498	0.4833		○	○	○
STK4	BC005231	*Homo sapiens* serine/threonine kinase 4, mRNA (cDNA clone IMAGE:3950315), complete cds.	0.4024	0.4833	○	○	○	
SMAD2	NM_005901	*Homo sapiens* SMAD family member 2 (SMAD2), transcript variant 1	0.3846	0.4833		○	○	○
FGFR2	NM_022970	*Homo sapiens* fibroblast growth factor receptor 2 (bacteria-expressed kinase, keratinocyte growth factor receptor, craniofacial dysostosis 1, Crouzon syndrome, Pfeiffer syndrome, Jackson–Weiss syndrome; FGFR2), transcript variant 2, mRNA	0.3038	0.4833			○	○
WNT9A	NM_003395	*Homo sapiens* wingless-type MMTV integration site family, member 9A (WNT9A)	0.3830	0.7799			○	
WNT1	NM_005430	*Homo sapiens* wingless-type MMTV integration site family, member 1 (WNT1)	0.4226	0.7799			○	
COL4A6	NM_033641	*Homo sapiens* collagen, type IV, α 6 (COL4A6), transcript variant B	0.1932	0.7799				○
PIK3CD	NM_005026	*Homo sapiens* phosphoinositide-3-kinase, catalytic, delta polypeptide (PIK3CD)	0.4580	0.7799				○
DAPK2	NM_014326	*Homo sapiens* death-associated protein kinase 2 (DAPK2)	0.3810	0.7799	○	○		○
FGF6	NM_020996	*Homo sapiens* fibroblast growth factor 6 (FGF6)	0.3913	0.7799			○	

(Continued on the following page)

Published OnlineFirst March 27, 2012; DOI:10.1158/1078-0432.CCR-11-1078

Table 2. Genes downregulated in cancer stroma, which are putative targets of miR-17-92a and/or miR-25-106b clusters (Cont'd)

Gene symbol	Genbank accession	Description	Fold Change[a]	Q (%)[a]	miR-17/20a/ 106b/93 target[b]	miR-18a target[b]	miR-19a/ 19b target[b]	miR-92a/25 target[b]
PLD1	NM_002662	*Homo sapiens* phospholipase D1, phosphatidylcholine specific (PLD1)	0.4685	0.7799	○	○	○	
FASLG	NM_000639	*Homo sapiens* Fas ligand (TNF superfamily, member 6; FASLG)	0.4284	1.2419	○	○	○	○
RUNX1	X90978	*Homo sapiens* mRNA for an acute myeloid leukaemia protein (1,793 bp)	0.4519	1.2419	○	○		
SMAD3	U68019	*Homo sapiens* mad protein homolog (hMAD-3) mRNA, complete cds	0.4943	1.2419		○		
LAMA3	NM_000227	*Homo sapiens* laminin, alpha 3 (LAMA3), transcript variant 2	0.4329	1.2419	○			
DCC	NM_005215	*Homo sapiens* deleted in colorectal carcinoma (DCC)	0.4342	1.2419			○	
WNT7B	NM_058238	*Homo sapiens* wingless-type MMTV integration site family, member 7B (WNT7B)	0.4704	1.2419	○	○	○	
FGF5	NM_004464	*Homo sapiens* fibroblast growth factor 5 (FGF5), transcript variant 1	0.4823	2.2195	○			○
HHIP	AK074711	*Homo sapiens* cDNA FLJ90230 fis, clone NT2RM2000410.	0.4494	3.4908				○
KEGG 04514 :Cell adhesion molecules (CAM)								
CNTN2	NM_005076	*Homo sapiens* contactin 2 (axonal; CNTN2)	0.1659	0.0748	○	○	○	
ALCAM	NM_001627	*Homo sapiens* activated leukocyte cell adhesion molecule (ALCAM)	0.2975	0.1256		○		
CD22	NM_001771	*Homo sapiens* CD22 molecule (CD22)	0.1359	0.1256			○	
SPN	NM_001030288	*Homo sapiens* sialophorin (leukosialin, CD43; SPN), transcript variant 1	0.3110	0.2025	○	○		○
CLDN18	NM_016369	*Homo sapiens* claudin 18 (CLDN18), transcript variant 1	0.3400	0.2025	○	○		
CNTNAP2	NM_014141	*Homo sapiens* contactin-associated protein-like 2 (CNTNAP2)	0.3082	0.3097	○			○
CLDN19	NM_148960	*Homo sapiens* claudin 19 (CLDN19)	0.3840	0.4833	○	○	○	○
PTPRC	NM_002838	*Homo sapiens* protein tyrosine phosphatase, receptor type, C (PTPRC), transcript variant 1	0.3629	0.7799				○
NRXN1	NM_004801	*Homo sapiens* neurexin 1 (NRXN1), transcript variant alpha	0.3674	0.7799		○		
CD8A	NM_001768	*Homo sapiens* CD8a molecule (CD8A), transcript variant 1	0.4033	1.2419		○		
CLDN16	NM_006580	*Homo sapiens* claudin 16 (CLDN16)	0.4543	1.2419		○		
CNTNAP1	NM_003632	*Homo sapiens* contactin-associated protein 1 (CNTNAP1)	0.4725	1.2419		○		
NCAM1	NM_000615	*Homo sapiens* neural cell adhesion molecule 1 (NCAM1), transcript variant 1	0.4247	1.2419			○	
CD28	NM_006139	*Homo sapiens* CD28 molecule (CD28)	0.4997	2.2195	○	○	○	

(Continued on the following page)

Published OnlineFirst March 27, 2012; DOI:10.1158/1078-0432.CCR-11-1078

Table 2. Genes downregulated in cancer stroma, which are putative targets of miR-17-92a and/or miR-25-106b clusters (Cont'd)

Gene symbol	Genbank accession	Description	Fold Change[a]	Q (%)[a]	miR-17/20a/ 106b/93 target[b]	miR-18a target[b]	miR-19a/ 19b target[b]	miR-92a/25 target[b]
L1CAM	NM_000425	*Homo sapiens* L1 cell adhesion molecule (L1CAM), transcript variant 1	0.4938	3.4908	○	○	○	
WNT9A	NM_003395	*Homo sapiens* wingless-type MMTV integration site family, member 9A (WNT9A)	0.3830	0.7799			○	
WNT1	NM_005430	*Homo sapiens* wingless-type MMTV integration site family, member 1 (WNT1)	0.4226	0.7799			○	
COL4A6	NM_033641	*Homo sapiens* collagen, type IV, alpha 6 (COL4A6), transcript variant B	0.1932	0.7799				○
PIK3CD	NM_005026	*Homo sapiens* phosphoinositide-3-kinase, catalytic, delta polypeptide (PIK3CD)	0.4580	0.7799				○
DAPK2	NM_014326	*Homo sapiens* death-associated protein kinase 2 (DAPK2)	0.3810	0.7799	○	○		○
FGF6	NM_020996	*Homo sapiens* fibroblast growth factor 6 (FGF6)	0.3913	0.7799			○	
PLD1	NM_002662	*Homo sapiens* phospholipase D1, phosphatidylcholine-specific (PLD1)	0.4685	0.7799	○	○	○	
FASLG	NM_000639	*Homo sapiens* Fas ligand (TNF superfamily, member 6; FASLG)	0.4284	1.2419	○	○	○	○
RUNX1	X90978	*Homo sapiens* mRNA for an acute myeloid leukaemia protein (1,793 bp).	0.4519	1.2419	○	○		
SMAD3	U68019	*Homo sapiens* mad protein homolog (hMAD-3)	0.4943	1.2419		○		
LAMA3	NM_000227	*Homo sapiens* laminin, alpha 3 (LAMA3), transcript variant 2	0.4329	1.2419	○			
DCC	NM_005215	*Homo sapiens* deleted in colorectal carcinoma (DCC)	0.4342	1.2419			○	
WNT7B	NM_058238	*Homo sapiens* wingless-type MMTV integration site family, member 7B (WNT7B)	0.4704	1.2419	○	○	○	
FGF5	NM_004464	*Homo sapiens* fibroblast growth factor 5 (FGF5), transcript variant 1	0.4823	2.2195	○			○
HHIP	AK074711	*Homo sapiens* cDNA FLJ90230 fis, clone NT2RM2000410.	0.4494	3.4908				○

NOTE: KEGG (ref. 18).

[a]Fold change < 0.50, Q < 0.05

[b]Based on the computational analysis by TargetScan (ref. 19, 20). Genes which are targets of each miRNA are marked with circle.

previously reported tumor-suppressive miRNAs, such as the *miR-192-miR-194* cluster, *miR-215*, *miR-29c*, *miR-26b*, and *let-7g* were all downregulated in cancer stromal tissues compared with normal stromal tissues (Supplementary Table S3) (22, 23). Downregulation of tumor-suppressive miRNAs in cancer stroma as well as upregulation of oncogenic miRNAs in cancer stroma indicated that alterations of miRNA expression in stromal tissues are similar to that in epithelial tissues.

Comparison of miRNA expression status in cancer stroma and cancer epithelium

Significantly upregulated or downregulated miRNAs in cancer stroma compared with cancer epithelium are listed in Supplementary Table S4A and S4B.

Discussion

In this study, we analyzed expression levels of miRNAs expressed in cancer stroma and revealed that many

Published OnlineFirst March 27, 2012; DOI:10.1158/1078-0432.CCR-11-1078

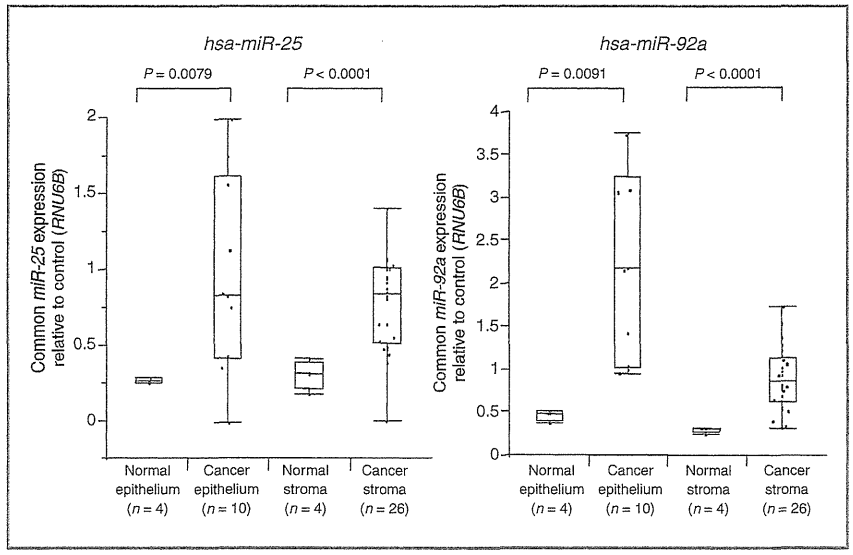

Figure 3. Expression of *miR-25* (left) and *miR-92a* (right) analyzed by quantitative RT-PCR in epithelium and stroma of cancer and normal tissue. Dots, expression of each sample; horizontal line, median; box, 25th through 75th percentile; error bars, range. Normal epithelium: $n = 4$, cancer epithelium: $n = 10$, normal stroma: $n = 4$, cancer stroma: $n = 26$.

oncogenic miRNAs including *miR-21* (24), *miR-221* (25), and almost all components of the *miR-17-92a* cluster and its homolog, and the *miR-106b-25* cluster were upregulated in cancer stroma compared with normal stroma (Table 1). Previous reports showed that the *miR-17-92a* cluster is upregulated in lung cancer, colorectal cancer, lymphoma, multiple myeloma, and medulloblastoma, whereas the *miR-106b-25* cluster is upregulated in gastric, colon, and prostate cancer, neuroblastoma, and multiple myeloma (9, 26, 27). Importantly, the expression of these miRNAs in stromal tissues had not been explored. We focused on these well-characterized miRNAs which are upregulated in cancer stroma as well as epithelial tissues.

The reason for the upregulation of such oncogenic miRNAs in stromal tissue is still unclear. However, previous studies have revealed genetic alterations such as LOH of cancer stromal cells (28) or epigenetic modification of cancer-associated fibroblasts (CAF; ref. 29). Hence, genetic or epigenetic changes of cancer stromal cells could be one explanation for this, although it remains controversial. Another possibility is intercellular transfer or penetration of miRNAs. It has been shown that secreted miRNAs from donor cells are transferred to and function in recipient cells. Some reports have shown that miRNAs are transferred in exosomes, vesicles of endocytic origin (30). If this occurred between cancer cells and stromal cells, profiles of miRNAs could become similar in both. We revealed that oncogenic miRNAs such as *miR-135b*, *miR-221*, and the *miR-17-92a* cluster were expressed at relatively higher levels in cancer epithelium than in stroma (Supplementary Table S4B). These findings suggest that upregulation of such oncogenic miRNAs in cancer stroma follows the upregulation of oncogenic miRNA in epithelium during carcinogenesis and cancer progression. However, further studies are required to confirm the interaction between cancer and its stroma.

Recently, Mestdagh and colleagues reported that the *miR-17-92* miRNA cluster regulated key components of the TGFβ pathway such as *SMAD2*, *SMAD4*, and *TGFBR2* in neuroblastoma (31). With regard to epithelial–mesenchymal interactions, Bhowmick and colleagues showed that ablation of *TGFBR2* in stromal tissue can lead to carcinogenesis and cancer progression *in vivo* (3). In our data, *TGFBR2*, *SMAD2*, and *SMAD3*, which are putative targets of the *miR-17-92a* and *miR-106b-25* cluster, were shown to be significantly repressed in cancer stroma (Table 2 and Table 3). These results suggest that, at least in part, inhibition of the TGFβ pathway in stromal tissue is associated with tumorigenesis and cancer progression. However, the putative miRNA target gene pathways we showed in this study have not been experimentally established, therefore, further exploration is needed to confirm that they function in stromal tissue.

Clinicopathologic analysis showed that miRNAs expression in stromal tissue is associated with the malignant potential of cancer (Table 4 and Table 5). High expression of *miR-25* was associated with venous invasion, and *miR-92a* with lymphatic and venous invasion and liver metastasis. These data indicate that miRNA expression in stroma as well as in the epithelium can influence tumor aggressiveness in colorectal cancer. Lymphatic or venous invasion occurs dominantly in stromal tissue; therefore these results are entirely reasonable. Although validation in a larger number of samples is required in future studies, our data indicate the potential clinical significance of miRNAs in cancer stroma.

Stromal tissues are constituted by various kinds of cells, including immune cells, endothelial cells, and fibroblasts. Previous reports suggested CAF or tumor-associated

Published OnlineFirst March 27, 2012; DOI:10.1158/1078-0432.CCR-11-1078

Table 3. Highly inverse-correlated miRNA and putative target gene pairs

miRNA name	mRNA name	Genbank accession	Description	correlation coefficient[a]	P[a]	Pathway (KEGG)[b]
hsa-miR-17	ACPP	NM_001099	Acid phosphatase, prostate	−0.8549	0.0002	00361: gamma-Hexachlorocyclohexane degradation, 00740: Riboflavin metabolism
hsa-miR-18a	HTR1D	NM_000864	5-Hydroxytryptamine (serotonin) receptor 1D	−0.8467	0.0003	04080: Neuroactive ligand–receptor interaction
hsa-miR-17	DAPK2	NM_014326	Death-associated protein kinase 2	−0.8073	0.0009	05200: Pathways in cancer, 05219: Bladder cancer
hsa-miR-17	LY75	NM_002349	Lymphocyte antigen 75	−0.8072	0.0009	
hsa-miR-17	TRIM7	NM_203297	Tripartite motif-containing 7	−0.7794	0.0017	
hsa-miR-19b	CASP7	NM_033338	Caspase 7, apoptosis-related cysteine peptidase	−0.7728	0.0020	04210: Apoptosis, 05010: Alzheimer's disease
hsa-miR-17	SHROOM1	NM_133456	shroom family member 1	−0.7553	0.0028	
hsa-miR-19a	PDE11A	NM_016953	Phosphodiesterase 11A	−0.7406	0.0038	00230: Purine metabolism
hsa-miR-20a	SYT13	NM_020826	Synaptotagmin XIII	−0.7385	0.0039	
hsa-miR-18a	PDE11A	NM_016953	Phosphodiesterase 11A	−0.7377	0.0040	00230: Purine metabolism
hsa-miR-18a	SLC18A1	NM_003053	Solute carrier family 18 (vesicular monoamine), member 1	−0.7342	0.0043	05012: Parkinson's disease
hsa-miR-19a	CLIC5	NM_016929	Chloride intracellular channel 5	−0.7231	0.0052	
hsa-miR-19a	ARFIP1	NM_001025595	ADP-ribosylation factor interacting protein 1	−0.7229	0.0052	
hsa-miR-19a	KCNV1	NM_014379	Potassium channel, subfamily V, member 1	−0.7190	0.0056	
hsa-miR-18a	MYO7B	BC035615	Myosin VIIB	−0.7151	0.0060	
hsa-miR-17	PKDREJ	NM_006071	Polycystic kidney disease (polycystin) and REJ homolog (sperm receptor for egg jelly homolog, sea urchin)	−0.7108	0.0065	
hsa-miR-19a	STX18	NM_016930	syntaxin 18	−0.7068	0.0069	04130: SNARE interactions in vesicular transport
hsa-miR-17	TRIM68	NM_018073	Tripartite motif-containing 68	−0.7058	0.0070	
hsa-miR-18a	SLC35D2	NM_007001	Solute carrier family 35, member D2	−0.7051	0.0071	
hsa-miR-17	TCF7	NM_003202	Transcription factor 7 (T-cell specific, HMG box)	−0.7023	0.0074	04310: Wnt signaling pathway, 04520: Adherens junction, 04916: Melanogenesis, 05200: Pathways in cancer, 05210: Colorectal cancer, 05213: Endometrial cancer, 05215: Prostate cancer, 05216: Thyroid cancer, 05217: Basal cell carcinoma, 05221: Acute myeloid leukemia, 05412: Arrhythmogenic right ventricular cardiomyopathy (ARVC)

(Continued on the following page)

Published OnlineFirst March 27, 2012; DOI:10.1158/1078-0432.CCR-11-1078

Table 3. Highly inverse-correlated miRNA and putative target gene pairs (Cont'd)

miRNA name	mRNA name	Genbank accession	Description	correlation coefficient[a]	P[a]	Pathway (KEGG)[b]
hsa-miR-18a	SLC5A9	NM_001011547	Solute carrier family 5 (sodium/glucose cotransporter), member 9	−0.7009	0.0076	
hsa-miR-19a	ABLIM1	NM_001003408	Actin binding LIM protein 1	−0.6966	0.0082	04360: Axon guidance
hsa-miR-18a	CASP7	NM_033338	Caspase 7, apoptosis-related cysteine peptidase	−0.6960	0.0082	04210: Apoptosis, 05010: Alzheimer's disease
hsa-miR-20a	H2AFJ	NM_177925	H2A histone family, member J	−0.6939	0.0085	05322: Systemic lupus erythematosus
hsa-miR-17	SLC39A8	NM_022154	Solute carrier family 39 (zinc transporter), member 8	−0.6910	0.0089	
hsa-miR-17	CLIC5	NM_016929	Chloride intracellular channel 5	−0.6887	0.0092	
hsa-miR-20a	KIAA0319	NM_014809	KIAA0319	−0.6783	0.0108	
hsa-miR-19a	CEACAM8	NM_001816	Carcinoembryonic antigen-related cell adhesion molecule 8	−0.6751	0.0114	
hsa-miR-19a	TRIM68	NM_018073	Tripartite motif-containing 68	−0.6714	0.0120	
hsa-miR-19a	SFT2D3	NM_032740	SFT2 domain containing 3	−0.6684	0.0125	
hsa-miR-17	GGT6	NM_153338	γ-glutamyltransferase 6	−0.6676	0.0127	00430: Taurine and hypotaurine metabolism, 00450: Selenoamino acid metabolism, 00460: Cyanoamino acid metabolism, 00480: Glutathione metabolism, 00590: Arachidonic acid metabolism, 01100: Metabolic pathways
hsa-miR-20a	XDH	NM_000379	Xanthine dehydrogenase	−0.6673	0.0127	00230: Purine metabolism, 00232: Caffeine metabolism, 00983: Drug metabolism–other enzymes, 01100: Metabolic pathways
hsa-miR-20a	PPARA	NM_005036	Peroxisome proliferator-activated receptor α	−0.6654	0.0131	03320: PPAR signaling pathway, 04920: Adipocytokine signaling pathway
hsa-miR-17	C2orf15	NM_144706	Chromosome 2 open reading frame 15	−0.6653	0.0131	
hsa-miR-17	GK5	BX648681	Glycerol kinase 5 (putative)	−0.6634	0.0134	
hsa-miR-17	SIDT1	NM_017699	SID1 transmembrane family, member 1	−0.6619	0.0137	
hsa-miR-25	ATP10B	AB018258	ATPase, class V, type 10B	−0.6605	0.0140	
hsa-miR-17	TMC5	NM_024780	Transmembrane channel-like 5	−0.6590	0.0143	
hsa-miR-18a	ALDH1A2	NM_170697	Aldehyde dehydrogenase 1 family, member A2	−0.6586	0.0144	00830: Retinol metabolism, 01100: Metabolic pathways
hsa-miR-17	INADL	NM_176877	InaD-like (*Drosophila*)	−0.6516	0.0158	04530: Tight junction

NOTE: Based on the computational analysis by TargetScan (ref. 19, 20).
[a]Correlation coefficient <−0.65, $P < 0.05$ Ranked by correlation coefficient.
[b]KEGG, kyoto encyclopedia of genes and genomes (ref. 18).

Published OnlineFirst March 27, 2012; DOI:10.1158/1078-0432.CCR-11-1078

Table 4. *miR-25* expression in cancer stroma and clinocopathologic factors

Factors	High expression ($n = 18$)	Low expression ($n = 6$)	*P*
Age (mean ± SD)	62.8 ± 2.95	66.5 ± 5.11	0.54
Sex			
Male	9	5	0.13
Female	9	1	
Histologic grade			
Well/moderately	11	4	0.81
Poorly/others	7	2	
Size			
50 mm≥ (small)	10	4	0.63
51 mm≤ (large)	8	2	
Depth of tumor invasion[a]			
m, sm, mp[a]	6	2	1
ss, se, si	12	4	
Lymph node metastasis			
Absent	13	2	0.092
Present	5	4	
Lymphatic invasion			
Absent	6	4	0.15
Present	12	2	
Venous invasion			
Absent	4	4	0.046[b]
Present	14	2	
Liver metastasis			
Absent	15	5	1
Present	3	1	
Dukes stage			
AB	11	2	0.24
CD	7	4	

[a]Tumor invasion of mucosa (m), submucosa (sm), muscularis propria (mp), subserosa (ss), penetration of serosa (se), and invasion of adjacent strucures (si)
[b]P < 0.05.

Table 5. *miR-92a* expression in cancer stroma and clinocopathologic factors

Factors	High expression ($n = 6$)	Low expression ($n = 18$)	*P*
Age (mean ± SD)	72.0 ± 4.74	61.0 ± 2.74	0.057
Sex			
Male	4	10	0.63
Female	2	8	
Histologic grade			
Well/moderately	4	11	0.81
Poorly/others	2	7	
Size			
50 mm> (small)	3	11	0.63
51 mm< (large)	3	7	
Depth of tumor invasion[a]			
m, sm, mp[a]	1	7	0.3
ss, se, si	5	11	
Lymph node metastasis			
Absent	3	12	0.47
Present	3	6	
Lymphatic invasion			
Absent	0	10	0.0050[b]
Present	6	8	
Venous invasion			
Absent	0	8	0.016[b]
Present	6	10	
Liver metastasis			
Absent	3	17	0.018[b]
Present	3	1	
Dukes stage			
AB	2	11	0.24
CD	4	7	

[a]Tumor invasion of mucosa (m), submucosa (sm), muscularis propria (mp), subserosa (ss), penetration of serosa (se), and invasion of adjacent strucures (si).
[b]*P* < 0.05.

macrophage could enhance tumor progression and metastasis (4, 32), and Vermeulen and colleagues showed that myofibroblasts play a role in the maintenance of cancer stem cell properties (33). In this study, we analyzed unsorted samples of stromal tissue, therefore the miRNA profiling for each cell type was not available. Sorting according to surface antigen, such as CD31 for endothelial cells or CD14 for macrophage, will be required for cell type–specific investigations in future studies.

Our findings suggest the possibility that oncogenic miRNAs including the *miR-17-92a* and *miR-25-106b* clusters in colorectal cancer stromal tissues are functionally associated with cancer progression. Because our results are based on microarray data derived from a small sample size, further validation is required.

Disclosure of Potential Conflicts of Interest

No potential conflicts of interest were disclosed.

Authors' Contributions

Conception and design: N. Nishida, M. Nagahara, K. Mimori, H. Ishii, M. Mori
Development of methodology: N. Nishida, M. Nagahara, F. Tanaka, H. Ishii, M. Mori
Acquisition of data (provided animals, acquired and managed patients, provided facilities, etc.): N. Nishida, H. Ishii, M. Mori
Analysis and interpretation of data (e.g., statistical analysis, biostatistics, computational analysis): N. Nishida, T. Sato, H. Ishii, M. Mori
Writing, review, and/or revision of the manuscript: N. Nishida, K. Mimori, T. Sudo, F. Tanaka, H. Ishii, M. Mori
Administrative, technical, or material support (i.e., reporting or organizing data, constructing databases): N. Nishida, T. Sudo, H. Ishii, M. Mori
Study supervision: N. Nishida, K. Mimori, F. Tanaka, K. Shibata, K. Sugihara, Y. Doki, M. Mori

Published OnlineFirst March 27, 2012; DOI:10.1158/1078-0432.CCR-11-1078

Acknowledgments

The authors thank T. Shimooka, K. Ogata, M. Kasagi, and T. Kawano for their excellent technical assistance.

Grant Support

This work was supported in part by the following grants and foundations: CREST, Japan Science and Technology Agency (JST); Japan Society for the Promotion of Science (JSPS) grant-in-aid for Scientific Research: 21679006, 20390360, 20590313, 20591547, 21591644, 21592014, 20790960, 21791297, 21229015, 20659209, and 20012039; NEDO (New Energy and Industrial Technology Development Organization) Technological Development for Chromosome Analysis; The Ministry of Education, Culture, Sports, Science and Technology of Japan for Scientific Research on Priority Areas, Cancer Translational Research Project, Japan; and LS094, Bureau of Science, Technology and Innovation Policy, Cabinet Office, Government Of Japan.

The costs of publication of this article were defrayed in part by the payment of page charges. This article must therefore be hereby marked *advertisement* in accordance with 18 U.S.C. Section 1734 solely to indicate this fact.

Received April 22, 2011; revised March 14, 2012; accepted March 15, 2012; published OnlineFirst March 27, 2012.

References

1. Kurose K, Gilley K, Matsumoto S, Watson PH, Zhou XP, Eng C. Frequent somatic mutations in PTEN and TP53 are mutually exclusive in the stroma of breast carcinomas. Nat Genet 2002;32:355–7.
2. Trimboli AJ, Cantemir-Stone CZ, Li F, Wallace JA, Merchant A, Creasap N, et al. Pten in stromal fibroblasts suppresses mammary epithelial tumours. Nature 2009;461:1084–91.
3. Bhowmick NA, Chytil A, Plieth D, Gorska AE, Dumont N, Shappell S, et al. TGF-beta signaling in fibroblasts modulates the oncogenic potential of adjacent epithelia. Science 2004;303:848–51.
4. Kalluri R, Zeisberg M. Fibroblasts in cancer. Nat Rev Cancer 2006;6:392–401.
5. Sund M, Kalluri R. Tumor stroma derived biomarkers in cancer. Cancer Metastasis Rev 2009;28:177–83.
6. Finak G, Bertos N, Pepin F, Sadekova S, Souleimanova M, Zhao H, et al. Stromal gene expression predicts clinical outcome in breast cancer. Nat Med 2008;14:518–27.
7. Fukino K, Shen L, Patocs A, Mutter GL, Eng C. Genomic instability within tumor stroma and clinicopathological characteristics of sporadic primary invasive breast carcinoma. JAMA 2007;297:2103–11.
8. Bartel DP. MicroRNAs: target recognition and regulatory functions. Cell 2009;136:215–33.
9. Nicoloso MS, Spizzo R, Shimizu M, Rossi S, Calin GA. MicroRNAs–the micro steering wheel of tumour metastases. Nat Rev Cancer 2009;9:293–302.
10. Nishida K, Mine S, Utsunomiya T, Inoue H, Okamoto M, Udagawa H, et al. Global analysis of altered gene expressions during the process of esophageal squamous cell carcinogenesis in the rat: a study combined with a laser microdissection and a cDNA microarray. Cancer Res 2005;65:401–9.
11. Wang H, Ach RA, Curry B. Direct and sensitive miRNA profiling from low-input total RNA. RNA 2007;13:151–9.
12. Quackenbush J. Microarray data normalization and transformation. Nat Genet 2002;32 Suppl:496–501.
13. Lopez-Romero P, Gonzalez MA, Callejas S, Dopazo A, Irizarry RA. Processing of Agilent microRNA array data. BMC Res Notes 2010;3:18.
14. Lopez-Romero P. Pre-processing and differential expression analysis of Agilent microRNA arrays using the AgiMicroRna Bioconductor library. BMC Genomics 2011;12:64.
15. Brazma A, Hingamp P, Quackenbush J, Sherlock G, Spellman P, Stoeckert C, et al. Minimum information about a microarray experiment (MIAME)-toward standards for microarray data. Nat Genet 2001;29:365–71.
16. Nogales-Cadenas R, Carmona-Saez P, Vazquez M, Vicente C, Yang X, Tirado F, et al. GeneCodis: interpreting gene lists through enrichment analysis and integration of diverse biological information. Nucleic Acids Res 2009;37:W317–22.
17. Carmona-Saez P, Chagoyen M, Tirado F, Carazo JM, Pascual-Montano A. GENECODIS: a web-based tool for finding significant concurrent annotations in gene lists. Genome Biol 2007;8:R3.
18. Kanehisa M, Goto S. KEGG: kyoto encyclopedia of genes and genomes. Nucleic Acids Res 2000;28:27–30.
19. Lewis BP, Burge CB, Bartel DP. Conserved seed pairing, often flanked by adenosines, indicates that thousands of human genes are microRNA targets. Cell 2005;120:15–20.
20. Grimson A, Farh KK, Johnston WK, Garrett-Engele P, Lim LP, Bartel DP. MicroRNA targeting specificity in mammals: determinants beyond seed pairing. Mol Cell 2007;27:91–105.
21. Olive V, Jiang I, He L. mir-17-92, a cluster of miRNAs in the midst of the cancer network. Int J Biochem Cell Biol 2010;42:1348–54.
22. Spizzo R, Nicoloso MS, Croce CM, Calin GA. SnapShot: MicroRNAs in cancer. Cell 2009;137:586–586.e1.
23. Braun CJ, Zhang X, Savelyeva I, Wolff S, Moll UM, Schepeler T, et al. p53-Responsive micrornas 192 and 215 are capable of inducing cell cycle arrest. Cancer Res 2008;68:10094–104.
24. Asangani IA, Rasheed SA, Nikolova DA, Leupold JH, Colburn NH, Post S, et al. MicroRNA-21 (miR-21) post-transcriptionally downregulates tumor suppressor Pdcd4 and stimulates invasion, intravasation and metastasis in colorectal cancer. Oncogene 2008;27:2128–36.
25. le Sage C, Nagel R, Egan DA, Schrier M, Mesman E, Mangiola A, et al. Regulation of the p27(Kip1) tumor suppressor by miR-221 and miR-222 promotes cancer cell proliferation. EMBO J 2007;26:3699–708.
26. Petrocca F, Visone R, Onelli MR, Shah MH, Nicoloso MS, de Martino I, et al. E2F1-regulated microRNAs impair TGFbeta-dependent cell-cycle arrest and apoptosis in gastric cancer. Cancer Cell 2008;13:272–86.
27. Ventura A, Young AG, Winslow MM, Lintault L, Meissner A, Erkeland SJ, et al. Targeted deletion reveals essential and overlapping functions of the miR-17 through 92 family of miRNA clusters. Cell 2008;132:875–86.
28. Allinen M, Beroukhim R, Cai L, Brennan C, Lahti-Domenici J, Huang H, et al. Molecular characterization of the tumor microenvironment in breast cancer. Cancer Cell 2004;6:17–32.
29. Hu M, Yao J, Cai L, Bachman KE, van den Brule F, Velculescu V, et al. Distinct epigenetic changes in the stromal cells of breast cancers. Nat Genet 2005;37:899–905.
30. Valadi H, Ekstrom K, Bossios A, Sjostrand M, Lee JJ, Lotvall JO. Exosome-mediated transfer of mRNAs and microRNAs is a novel mechanism of genetic exchange between cells. Nat Cell Biol 2007;9:654–9.
31. Mestdagh P, Bostrom AK, Impens F, Fredlund E, Van Peer G, De Antonellis P, et al. The miR-17-92 microRNA cluster regulates multiple components of the TGF-beta pathway in neuroblastoma. Mol Cell 2010;40:762–73.
32. Qian BZ, Pollard JW. Macrophage diversity enhances tumor progression and metastasis. Cell 2010;141:39–51.
33. Vermeulen L, De Sousa EMF, van der Heijden M, Cameron K, de Jong JH, Borovski T, et al. Wnt activity defines colon cancer stem cells and is regulated by the microenvironment. Nat Cell Biol 2010;12:468–76.

Hypoxia and *TP53* deficiency for induced pluripotent stem cell-like properties in gastrointestinal cancer

HIROMITSU HOSHINO[1], HIROAKI NAGANO[1], NAOTSUGU HARAGUCHI[2], SHIMPEI NISHIKAWA[1], AKIRA TOMOKUNI[1], YOSHIHIRO KANO[1], TAKAHITO FUKUSUMI[1], TOSHIYUKI SAITO[3], MIYUKI OZAKI[2], DAISUKE SAKAI[2], TAROH SATOH[2], HIDETOSHI EGUCHI[1], MITSUGU SEKIMOTO[1], YUICHIRO DOKI[1,2], MASAKI MORI[1,2*] and HIDESHI ISHII[1-3*]

Departments of [1]Gastroenterological Surgery, [2]Frontier Science for Cancer and Chemotherapy, Osaka University Graduate School of Medicine, Suita, Osaka 565-0871; [3]Transcriptome Profiling Group, National Institute of Radiological Sciences, Research Center for Charged Particle Therapy, Chiba 263-8555, Japan

Received October 14, 2011; Accepted December 1, 2011

DOI: 10.3892/ijo.2012.1346

Abstract. Induced pluripotent stem (iPS)-like cancer cells (iPC) by the introduction of defined transcription factors reduce the prevalence of the malignant phenotype of digestive system cancer cells, but the induction efficiency is low. The role of hypoxia and *TP53* deficiency in iPC cell generation remain unclear. Cellular reprogramming was performed by retroviral infection with *OCT3/4, SOX2, KLF4* and *c-MYC* of wild-type HCT116 colorectal cancer cells and mutant *TP53*-deficient HCT116 cells. Cells were cultured in normoxia (21% O_2) or hypoxia (5% O_2) for 30 days after transduction, and the response to hypoxia and comparison of cellular proliferation, invasion and tumourigenesis before and after iPC cell generation were studied. iPC cell generation from wild-type HCT116 cells in hypoxia was approximately 4-times greater than in normoxia ($p<0.05$), and *TP53* deficiency increased conversion efficiency significantly in normoxia ($p<0.05$). Significant involvement of hypoxia-inducible factors was observed in an immature carbohydrate epitope, Tra-1-60$^+$, colony formation. Generated iPC cells exhibited multi-differentiation potential. Although the iPC cells in hypoxia exhibited reduced proliferation, invasiveness and tumourigenicity, *TP53* deficiency in iPC cells resulted in higher tumourigenicity than in wild-type cells. Both hypoxia and *TP53* deficiency increase iPC cell generation. *TP53* deficiency can also result in deleterious mutations, whereas hypoxia may impact molecular targets of epigenome normalisation.

Correspondence to: Professor Masaki Mori, Department of Gastroenterological Surgery, Osaka University Graduate School of Medicine, Yamadaoka 2-2, Suita, Osaka 565-0871, Japan
E-mail: mmori@gesurg.med.osaka-u.ac.jp

Professor Hideshi Ishii, Department of Frontier Science for Cancer and Chemotherapy, Osaka University Graduate School of Medicine, Yamadaoka 2-2 (E21-19), Suita, Osaka 565-0871, Japan
E-mail: hishii@gesurg.med.osaka-u.ac.jp

*Contributed equally

Key words: cancer reprogramming, epigenome normalisation, hypoxia, tumour suppressor genes

Introduction

Although disruption of the normal differentiation process is an important component of tumourigenesis (1) and is involved in leukaemogenesis (2) and the formation of other malignancies (3), not much is understood about the reversibility of this process. In general, genetic alterations such as mutations (substitutions of nucleotide sequences), amplifications and deletions, as well as recurring chromosomal aberrations are irreversible, whereas epigenetic alterations can be modified by pharmacological agents that target components of the epigenetic machinery (4). Since epigenetic modifications, including DNA methylation and histone modifications, substantially contribute to the tumour cell phenotype, the number of potential therapeutic targets has increased (5). Epigenome normalisation is a potential therapeutic approach for cancer treatment in the clinical setting and in translational aspects of epigenetic research (5).

An important discovery that has been reported is that complete reprogramming can be achieved by the introduction of defined transcription factors, Oct4 (also known as Pou5f1), Sox2, Klf4 and cMyc, from terminally differentiated somatic fibroblasts (6). Generation of induced pluripotent stem (iPS) cells is believed to require epigenetic modifications, but the precise mechanism is unknown (7). Recently, we showed that introducing defined factors in gastrointestinal cancer cells resulted in the acquisition of multi-differentiation potential, i.e. the gene expression profiles of mesoderm and ectoderm appeared in gastrointestinal cancer cells of endodermal origin [iPS-like cancer (iPC) cells] (8). Reprogramming of sensitised cancer cells in response to differentiation therapy suppressed tumourigenicity *in vivo* (8); this presumably involved reactivation of tumour suppressor genes at the *CDKN2b-CDKN2a* locus on chromosome 9p21 in humans (chromosome 4 in mice), a region that is frequently inactivated in cancer and

is involved in the reduction of chemosensitivity (9). Together, these findings strongly suggest that the magnitude of epigenetic modifications using iPS technology may be sufficient to reverse the differentiation programme and lead to a multipotent state as well as contribute to the suppression of biologically malignant phenotypes in cancer cells.

Recent studies have shown that silencing or absence of p53 significantly increases iPS cell generation (10-12). Another study demonstrated that hypoxia enhance iPS cell generation in humans and mice (13). Since p53 activation characterises cancer cells that survive in hypoxia (14,15), it is possible that reprogramming of cancer cells may be closely associated with the p53 and hypoxic pathways. Herein, we studied these pathways and demonstrated that although prolonged *in vitro* culture increased tumourigenic potential in *TP53*-deficient iPC cells, hypoxia and *TP53* deficiency enhances iPC cell generation. This suggests that *TP53* deficiency functions as a two-edged sword and that *TP53* is a candidate molecular marker for predicting the biological behaviour of reprogrammed cancer cells.

Materials and methods

Cell lines and culture. Wild-type (wt) and TP53-deficient colorectal cancer (CRC) cell lines, wt HCT116 cells and its homologous-recombination mutant, HCT116 p53-deficient (null) cells, were donated by Dr Bert Vogelstein (Johns Hopkins University, Baltimore, MD, USA), and other cancer cell lines were obtained from DS Pharma Biomedical Co., Ltd. (Osaka, Japan). Cell lines were maintained in Dulbecco's modified Eagle's medium (DMEM; Nacalai Tesque, Kyoto, Japan) supplemented with 10% foetal bovine serum (FBS) at 37˚C in a 5% humidified CO_2 atmosphere. Plasmids were purchased from Addgene (Cambridge, MA). Transfectants were grown in DMEM supplemented with 10% FBS and puromycin (2 μg/ml) and subsequently incubated in specific culture conditions as described previously (8). All retroviral transfections were performed using ViraDuctin Transduction kit (Cell Biolabs, San Diego, CA). Transfections with lentivirus were performed using the Virapower Lentiviral Packaging mix (Invitrogen, Carlsbad, CA). In brief, cancer cell lines were transfected with plasmids at a concentration of 4 μg/μl using Lipofectamine 2000 (Invitrogen) and incubated in glucose-free Opti-MEM (Invitrogen). These transfected cell lines were cultured in 21% or 5% CO_2. All experiments were performed at 50-70% cell confluence and results were confirmed in at least three independent experiments. All-in-one type fluorescence microscope (BZ-8000; Keyence, Osaka, Japan) with digital photographic capability was used to visualise cells at several magnifications. In the proliferation assay, growth rates of the cultured gastrointestinal cancer cell lines were measured by counting cells using Celltac (Nihon Kohden Co., Tokyo, Japan).

RNA preparation and real-time reverse transcription-polymerase chain reaction (qRT-PCR). Total RNA was prepared using TRIzol reagent (Invitrogen). RT was performed using SuperScript III RT kits (Invitrogen). To confirm PCR amplification, 25-35 cycles of PCR were performed using a PCR kit (Takara, Kyoto, Japan) on the GeneAmp PCR System 9600 (PE Applied Biosystems, Foster City, CA) in the following conditions: 95˚C for 10 sec, 60˚C for 10 sec and 72˚C for 60 sec. An 8-μl aliquot of each reaction mixture was size-fractionated in a 1.5% agarose gel and visualised by ethidium bromide staining. To confirm RNA quality, PCR amplification was performed for *GAPDH* using specific primers. For quantitative assessment, the gene expression was evaluated by qRT-PCR using a LightCycler TaqMan Master kit (Roche Diagnostics, Tokyo, Japan) for cDNA amplification of specific target genes. The expression of mRNA copies was normalised against *GAPDH* mRNA expression.

Reagents and antibodies. Antibodies against Nanog, Ssea-4, Tra-1-60, Tra-1-81 and Tra-2-49 (Chemicon International Inc., Temecula, CA) were used for immunocytology.

Invasion assay. Cell invasion was analysed using the CytoSelect assay kit according to the manufacturer's protocol (Cell Biolabs). Cells ($1.0x10^5$) in DMEM were placed on 8.0-μm pore-size membrane inserts in 96-well plates, and DMEM with 10% FBS was added to each well. After 24-h incubation at 37˚C in 5% CO_2, non-invading cells were removed from the top of the membrane chamber and cells on the underside of the membrane were completely dislodged by tilting the membrane chamber in cell detachment solution (Cell Biolabs). Lysis buffer/CyQuant GR dye solution (Cell Biolabs) was then added to each well, and fluorescence was determined at 480 or 520 nm using a plate reader to estimate the number of cells that had invaded the undersurface of the membrane. Each assay was performed in triplicate.

Tumourigenicity. Cells were subcutaneously inoculated into NOD/SCID mice. The tumour diameter and size were estimated using the following formula: size = $(\text{length})^2$ x (width)/2

Statistical analysis. For continuous variables, results are expressed as means ± standard errors. The relationship between the gene expression level and cell count was analysed by Chi-square and Wilcoxon rank tests. All data were analysed using JMP software (SAS Institute, Cary, NC). Differences with $p<0.05$ were considered statistically significant.

Results

Lentiviral- and retroviral-mediated iPS factor gene transfer. The expression profile of ES-like genes is reportedly associated with aggressive phenotypes observed in solid tumours (16). Considering that reprogramming induces the endogenous expression of ES-like genes, it is assumed that the expression of endogenous genes may be involved in reprogramming and some cancer cells with a relatively higher expression of endogenous ES-like genes may be sensitive to reprogramming induction. We quantitatively studied the expression of endogenous immature *NANOG* by qRT-PCR (data not shown), because *NANOG* is not included in exogenously mediated reprogramming vectors in the present experiment but is relevant to the immature status of iPS cells (6,17). The *NANOG* expression level in HCT116 p53 null cells was equal to that in PANC-1 cells, but compared with that in NTERA teratoma cells it was ~20% greater, while the expression in wt HCT116 cancer cell lines was relatively low (data not shown). We thus selected two cells each from wt HCT116 cells, its derivative

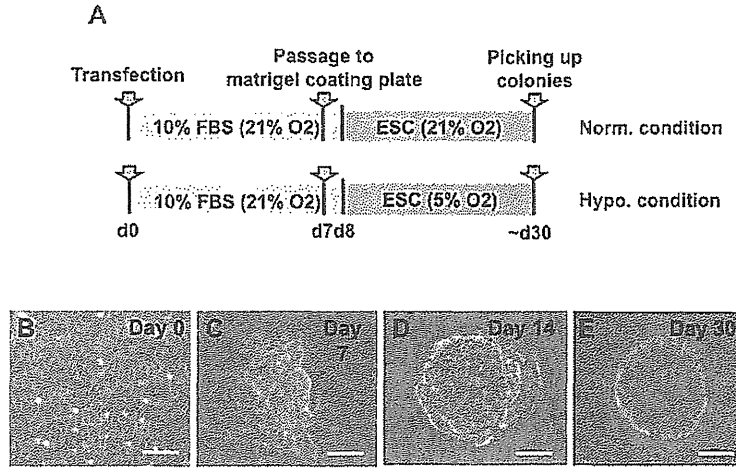

Figure 1. Retroviral- and lentiviral-mediated gene transfer of four iPS factor genes in gastrointestinal cancer cells. (A) Schematic representation of the experiment showing normoxia and hypoxia. (B-E) Morphological changes in iPC cells derived from pancreatic cancer wt HCT116 cells. (B) Day 0, (C) day 7, (D) day 14, (E) day 30 after transfection. Scale bar, 100 μm.

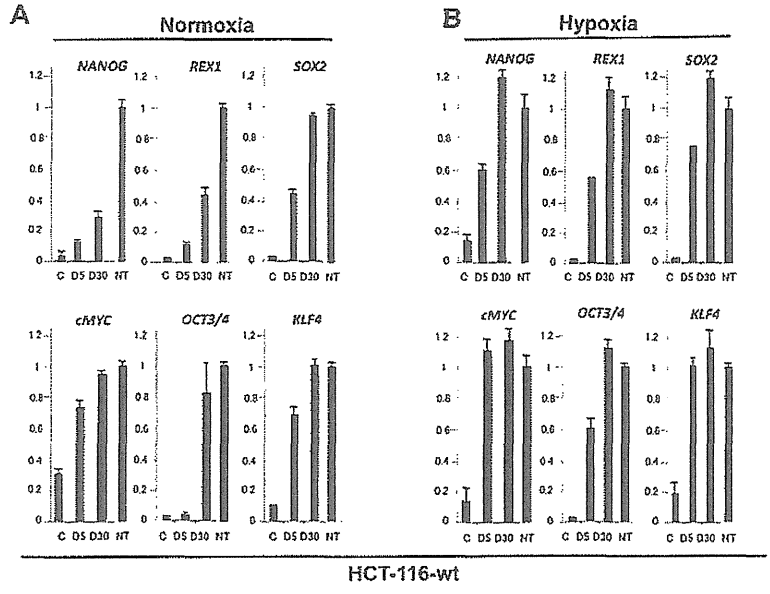

Figure 2. Exogenous and endogenous gene expression by iPS cells after retroviral- and lentiviral-mediated gene transfer in wt HCT116 cells. After viral vector-mediated gene transfer of the four defined factor genes *c-MYC, SOX2, OCT3/4* and *KLF4*, the expression of all exogenous and endogenous genes was assessed in normoxia (A) or hypoxia (B) on days 5 and 30 by qRT-PCR using specific primers.

line HCT116 p53 null cells and PANC-1 cells for comparison in subsequent experiments.

For the transfer of iPS factor genes, we infected cells on day 0 through lentiviral-mediated transfer of murine retroviral receptors followed by retroviral-mediated gene transfer of the four defined factor genes *c-MYC, SOX2, OCT3/4* and *KLF4*. On day 7, cells were transferred to ES culture medium in either hypoxia (5% O_2) or continuous normoxia (21% O_2) (Fig. 1A). The number of cells increased on day 7 and clear round colonies were formed by day 30 (representative data are shown in Fig. 1B-E). These induced cells were morphologically similar or indistinguishable from iPC cells derived from other gastrointestinal cancer cells (8) and were similar to iPS cells derived from terminally differentiated normal cells (7).

The expression in wt HCT116 and HCT116 p53 null cells of four exogenously introduced transgenes and endogenous genes in normoxia and hypoxia were analysed by qRT-PCR (Fig. 2, and data not shown). On day 5, the expression levels of exogenously introduced c-MYC, SOX2, OCT3/4 and KLF4 in wt HCT116 cells were 40%-80% and >60% and those of REX1 and NANOG, which were not introduced as transgenes, were ~10 and 60% of those in teratoma NTERA cells in normoxia and hypoxia, respectively (Fig. 2). These results suggested that compared with normoxia, hypoxia stimulates endogenous expression of ES-like genes, such as *REX1* and *NANOG*, and the relevance of this result was appreciable in assessment of four exogenously introduced transgenes and endogenous genes.

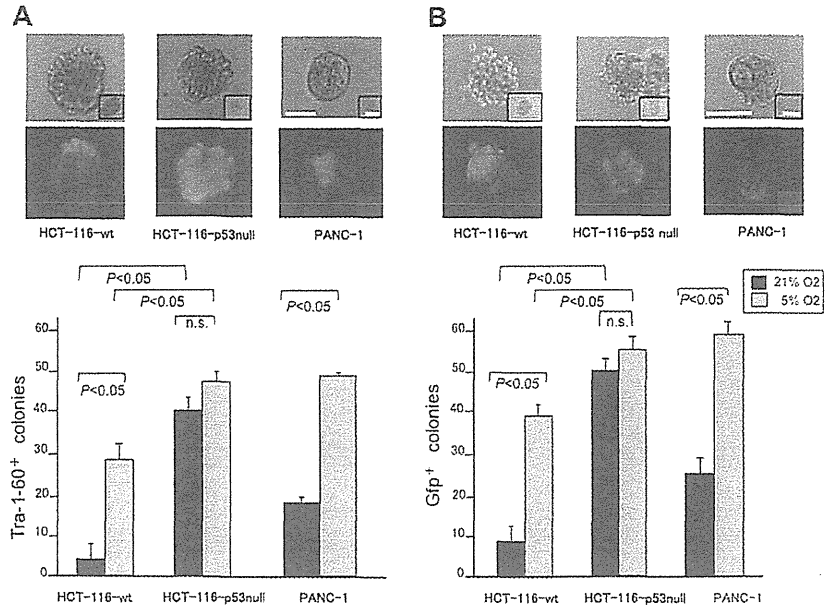

Figure 3. Effect of hypoxia on *TP53*-deficient cancer cells. The effects of reprogramming of wt HCT116, HCT116 p53 null and PANC-1 cells are shown by (A) immunostaining with anti-Tra-1-60 antibody or (B) observation of GFP-positive spheres under a fluorescence microscope on day 30. Reprogramming efficiency (percentage of Tra-1-60- or GFP-positive cells) in hypoxia (5% O_2) was higher than in normoxia (21% O_2). p-values are shown for each comparison. Scale bar, 50 μm.

On day 30, the expression levels of exogenously introduced *REX1* and *NANOG* were 30-40% and >100% and those of the endogenously introduced *c-MYC*, *SOX2* and *OCT3/4* were >80% of those in teratoma NTERA cells in normoxia and hypoxia, respectively (Fig. 2). By utilising specific primers, the assessment of exogenous expression levels on day 30 indicated that all transgenes in wt HCT116 cells had decreased to undetectable levels in normoxia and hypoxia, except for the expression levels of *c-MYC* in normoxia and hypoxia and *KLF4* in hypoxia, all of which persisted (data not shown). By day 30, the expression levels of all transgenes in HCT116 p53 null cells had decreased to undetectable levels in normoxia and hypoxia, except for the expression levels of *c-MYC* and *KLF4* in normoxia and hypoxia that persisted, and the expression levels were higher in hypoxia (data not shown). The overall trend of decreased exogenous gene expression levels is probably due to silencing of the introduced genes (7). Our data indicate that reprogramming factors elicited the specific activation of immature endogenous ES-like genes.

High expression of ES-like genes in hypoxia and TP53-deficient condition in iPC cells derived from gastrointestinal cancer. After the introduction of iPS factors, compared to the expression levels in wt HCT116 cells in normoxia and hypoxia, the expression levels of an immature carbohydrate epitope, Tra-1-60, in iPC cells derived from HCT116 p53 null cells was 8-times and 1.6-times greater ($p<0.05$, Fig. 3A), while those in PANC-1 cells was 2.4-times greater in hypoxia (5% O_2) than in normoxia (21% O_2) ($p<0.05$, Fig. 3A). These data indicate that p53-defiency induces reprogramming in normoxia, and to a lesser extent, in hypoxia, suggesting that the factors downstream of p53 signalling may be involved in increased reprogramming efficiency in hypoxia. On day 30, the increased expression of other immature carbohydrate epitopes and proteins, namely Tra-2-49, Tra-1-60, Tra-1-81, Ssea4 and Nanog, was confirmed by immunocytochemistry after the introduction of defined factors (data not shown).

For semi-quantitative analyses of *NANOG* promoter activity, the *NANOG* promoter fusion green fluorescent protein vector was co-transfected in iPC cell generation. The tracing study of *NANOG* promoter activity in iPC cells derived from HCT116 p53 null cells indicated that, compared with wt HCT116 cells, the endogenous *NANOG* promoter was activated after reprogramming in normoxia (5-times, $p<0.05$, Fig. 3B), and to a lesser extent in hypoxia (1.3-times, $p<0.05$, Fig. 3B). Similarly, *NANOG* promoter was activated in hypoxia in PANC-1 iPC cells (2.2-times, $p<0.05$, Fig. 3B). The data are consistent with the notion that reprogramming efficiency is increased by p53 deficiency and hypoxia in a common pathway. Although the observed *NANOG* reporter activity may reflect endogenous activity at a basal level (data not shown), the expression of Tra-1-60 seems to be more specific to reprogramming induction (6,17). We thus used Tra-1-60 to assess reprogramming in the following studies.

Previous studies indicated that the hypoxia-inducible factor (Hif) pathway plays a role in metabolic regulation of cancer, as in the p53 pathway (15). Thus, to determine whether Hif affects the downstream cellular response to reprogramming induction, we co-transfected cells with hydroxylation-defective active mutants *HIF1A-P402A/P564A* and *HIF2A-P405A/P531A*, which lack proline residues within the oxygen-dependent degradation domain. These residues are necessary for the interaction with von Hippel-Lindau tumour suppressor protein (pVHL) and their substitutions increase the stability of Hifs, because they resist proteasome-dependent degradation (15). qRT-PCR indicated that transgenes were detected for at least 5 days after transfection, which is the critical timeframe for reprogramming events involved in iPS generation (6,17). The Tra-1-60 expression data indicated that the introduction of

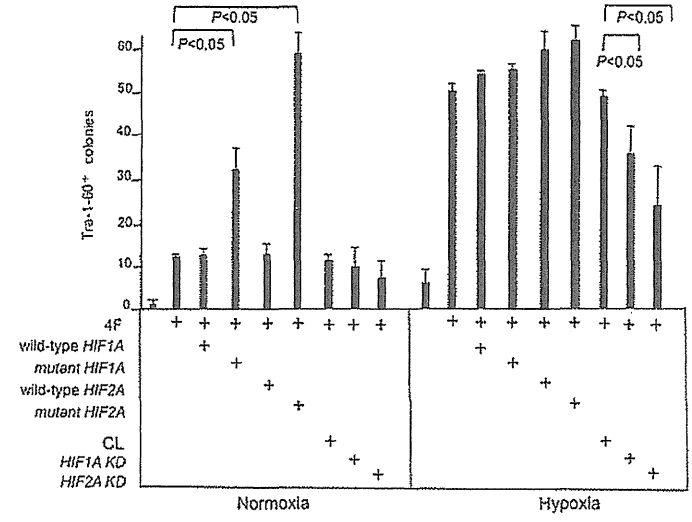

Figure 4. Efficiency of reprogramming induced by co-transfection with iPS factors and mutant *HIF* in wt HCT116 cells. Number of Tra-1-60$^+$ and GFP$^+$ clones as percentage of colonies on day 30 after gene transfer are shown. 4F, four factor genes *(c-MYC, SOX2, OCT3/4* and *KLF4)*; mutant *HIF1A*, the hydroxylation-defective mutant *HIF1A-P402A/P564A* lacking proline residues that are necessary for the interaction with pVHL and are refractory to proteasome-dependent degradation; mutant *HIF2A*, the hydroxylation-defective mutant *HIF2A-P405A/P531A*; *HIF1A KD*, lentiviral shRNA knockdown of *HIF1A*; *HIF2A KD*, lentiviral shRNA knockdown of the *HIF2A*; CL, lentiviral shRNA against luciferase as a control. p-values are shown for each comparison.

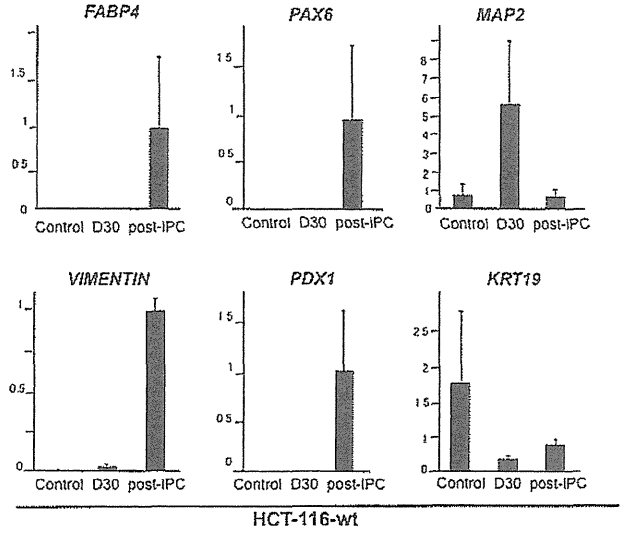

Figure 5. Multi-differentiation potential of iPC cells after reprogramming. After generating iPC cells from wt HCT116 cells in hypoxia (5% O_2), the expression levels of *FABP4, PAX6, MAP2, VIMENTIN, PDX1* and *KRT19* were analysed by qRT-PCR on day 30 (iPC; D30) or after subsequent differentiation-induction culture for 20 days (post-iPC).

HIF2A-P405A/P531A mutants, but not wild-type *HIF2A*, increased reprogramming efficiency in normoxia (4.8-times, p<0.05, Fig. 4), whereas the introduction of *HIF1A-P402A/P564A* mutants, but not wild-type *HIF1A*, increased reprogramming efficiency (2.7-times, p<0.05, Fig. 4).

In hypoxia, the expression of Tra-1-60 was increased regardless of whether wild-type or mutant *HIF1A* and *HIF2A* were co-transfected, indicating that hypoxia attenuated the effect of mutations in Hif proteins and that the Hif pathway plays a role in the increased reprogramming efficiency of cancer cells. To confirm these indications, we performed a knockdown experiment. The lentiviral shRNA transduction system indicated that knockdown lasting for at least 5 days resulted in reduced generation of Tra-1-60$^+$ cells in hypoxia. In other words, reprogramming efficiency was decreased after *HIF2A* knockdown (0.5-times, p<0.05) and *HIF1A* knockdown (0.75-times, p<0.05), but the knockdown effect was not detected in normoxia, supporting the notion that the Hif pathway plays a role in the efficiency of iPC cell generation in hypoxia. This suggests that the effect of hypoxia can be explained at least partially by the activation of the Hif2a pathway, and increased expressions in hypoxia can be explained by the activation of the Hif pathway, indicating that it is involved in the regulation of iPC cell generation.

Multi-differentiation potential of iPC cells. To assess the multi-differentiation potential of iPC cells, induced cells were subjected to *in vitro* induction of differentiation. Established iPC cells in ES culture medium were transferred to DMEM with 10% FBS (DMEM does not support growth of cells in an undifferentiated state), grown for 20 days to elicit differentiation (post-iPC cells) and their gene expression was then studied by qRT-PCR. The expression of *PDX1* (a transcription factor involved in pancreatic development), *VIMENTIN* (a mesenchymal marker) and *PAX6* (an ectoderm marker) markedly increased in post-iPC cells derived from wt HCT116 (Fig. 5) and HCT116 p53 null iPC cells (data not shown). The *MAP2* expression in post-iPC cells decreased, but remained detectable in wt HCT116 (Fig. 5) and HCT116 p53 null iPC cells (data not shown), although the expression was relatively high in wt HCT116 cells on day 30. Induction of a-Sma (muscle), Gfap (ectoderm), Vimentin, Keratin 19 (epithelial) and Tubb3 (ectoderm) proteins was confirmed by immunocytochemical staining with specific antibodies (data not shown). The data indicate that the four defined factor-induced reprogramming resulted in multi-differentiation potential in cancer cells. Next, a proliferation assay showed that cell growth was significantly

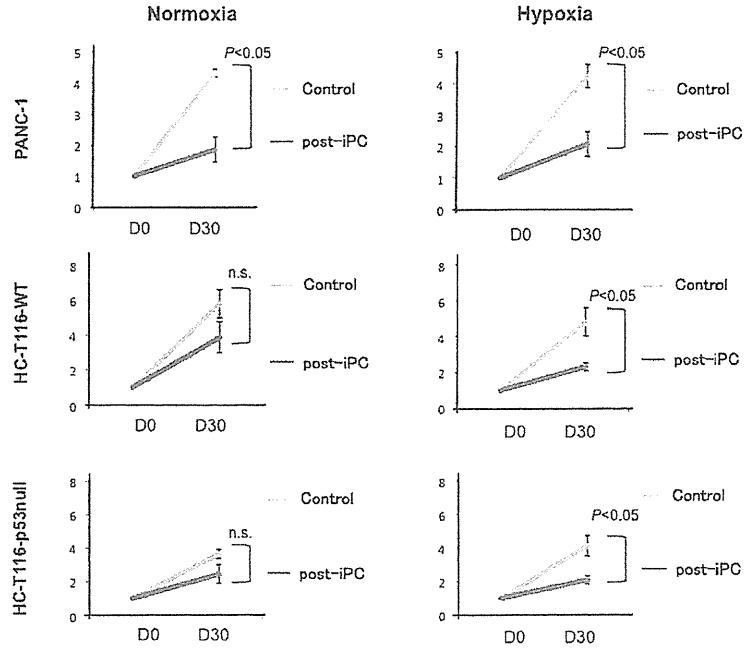

Figure 6. iPC cell proliferation assay. Control parental and iPC cells were derived from wt HCT116, HCT116 p53 null and PANC-1 cells in normoxia or hypoxia and subjected to a proliferation assay. Differences with $p<0.05$ were considered statistically significant.

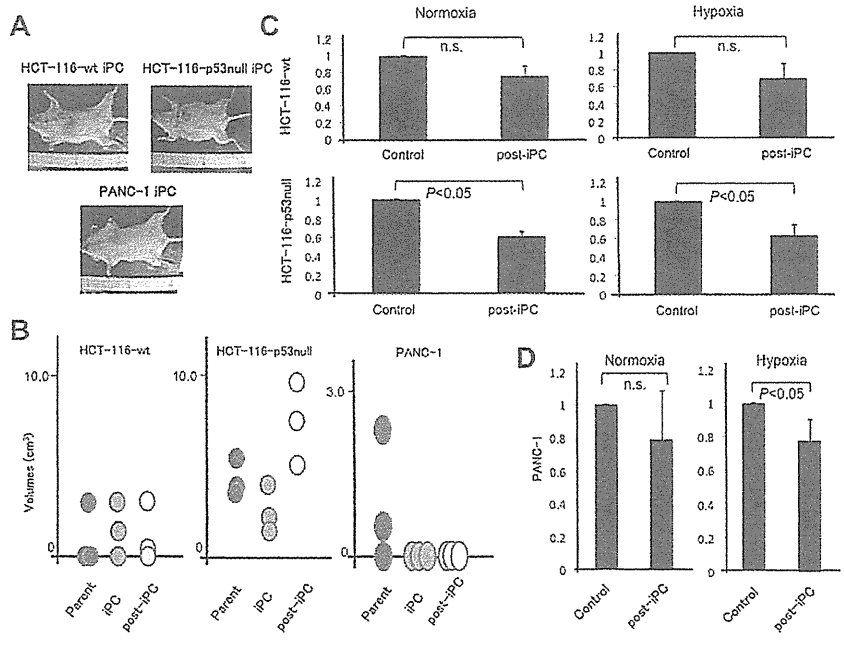

Figure 7. Tumourigenicity and invasion assay of iPC cells. (A and B) Tumourigenicity of parental wt HCT116, HCT116 p53 null and PANC-1 cells and the iPC and post-iPC cells derived from them. (C) Invasion assay of iPC cells derived from wt HCT116 and HCT116 p53 null cells in normoxia and hypoxia. (D) Invasion assay of PANC-1 iPC cells induced in normoxia and hypoxia. Differences with $p<0.05$ were considered statistically significant.

reduced in post-iPC cells derived from PANC-1 iPC cells, but not parental PANC-1 cells cultured in the same DMEM with 10% FBS, in both normoxia and hypoxia ($p<0.05$, Fig. 6). Cell growth was also significantly reduced in wt HCT116 and HCT116 p53 null cells induced in hypoxia ($p<0.05$) and, to a lesser extent, in normoxia (not significant; Fig. 6). The data suggested that reprogramming induced a distinct phenotype from parental cancer cells efficiently in hypoxia.

Tumourigenicity and invasion of iPC cells. iPC cells were inoculated into NOD/SCID mice and tumour formation was observed. The tumourigenicity of iPC and post-iPC cells derived from PANC-1 cells was reduced compared to that of parental PANC-1 cells (Fig. 7A and B). The tumourigenicity of iPC and post-iPC cells derived from wt HCT116 cells was comparable to that of parental cells. The tumourigenicity of iPC cells derived from HCT116 p53 null cells was also comparable with that of

parental HCT116 p53 null cells; however, post-iPC cells derived from HCT116 p53 null cells showed increased tumourigenicity. *In vitro* invasion assay indicated that tumourigenicity was reduced in iPC cells derived from hypoxia condition and, to a lesser extent, normoxia condition in both wt HCT116 and HCT116 p53 null cells (Fig. 7C), whereas in iPC cells derived from PANC-1 cells the reduction was greater in hypoxia than in normoxia (Fig. 7D). Thus, the present study indicates that induction of iPC cells in hypoxia could cause an enhanced reduction *in vitro*, while *in vivo* growth in *TP53*-deficient background might elicit aggressive transformation and a higher level of tumourigenicity.

Discussion

Tumours can originate from stem or progenitor cells and epigenetic alterations are involved in cellular differentiation as in *BCR/ABL* translocation-positive haematopoietic stem cells in chronic myelogenous leukaemia and Lgr5-positive stem cells in CRC (1-3). This suggests that possible corrections of the differentiation program, reversion of aggressive phenotypes or induction of apoptosis in cancer cells may be an ideal therapeutic approach. Reprogramming induction of differentiated cells by transfection of defined transcription factors considerably modifies the epigenetic machinery, but genetic alterations in cancer cannot, in principle, be corrected by the introduction of defined transcription factors. Cancer cells generally harbour genetic instability and the extent to which epigenetic modifications associated with reprogramming can modulate the biological behaviour of tumour cells remains debatable. The present study suggests that the remaining p53 allele in wt HCT116 cancer cells is involved in reprogramming regulation and that its deficiency may accelerate the reprogramming of cancer cells. Since the p53 pathway is altered in ~50% of cancer cells, such cells may be susceptible to reprogramming induction. Furthermore, the present data indicate that hypoxia enhances the reprogramming induction. Considering that cancer metabolism is adaptive to hypoxia glycolysis and that a significant fraction of cancer cells, including cancer stem cells, can presumably survive in hypoxia or in a hypoxic niche, at least two pathways, the Hif and p53 pathways, may be targeted to regulate reprogramming therapy for cancer.

The tumourigenicity assay of HCT116 p53 null cells indicated that post-iPC cells exhibited a high level of tumour formation *in vivo*, whereas an *in vitro* study demonstrated that post-iPC cells derived from HCT116 p53 null cells exhibited reduced invasive activity and a lower cell proliferation rate than control cells. Hypoxia elicited the reprogramming suggesting that the microenvironment of tumour tissues, such as vascularisation *in vivo*, might affect tumour activation and that tumour activation is not a cell-autonomous mechanism. The p53 protein has been shown to limit angiogenesis, at least partly, by interfering with the central regulators of hypoxia that mediate angiogenesis (reviewed in ref. 18). Tumours with inactivated tumour suppressor p53 function, approximately half of all tumours, appear more vascularised, are often more aggressive and are correlated with poor post-treatment prognosis. Thus, the loss of functional p53 during tumourigenesis represents an essential step in the switch in hypoxia to an angiogenic phenotype that characterises aggressive tumours (18). To inhibit malignant transformation observed in the reprogrammed *TP53*-deficient cancer cells (the present study) and in other cancer cells with gain-of-function mutations such as $TP53^{R175H}$ and $KRAS^{G12D}$ (19), we suggest that the combination of anti-angiogenic therapy and therapies targeting *TP53* deficiency may be beneficial. For example, anti-vascular endothelial growth factor receptor antibodies may suppress the deleterious effect of *TP53*-deficient reprogramming. We speculate that, although *TP53* overlapped with the hypoxia pathway, *TP53* may play a critical role in the surveillance of the malignant phenotype or deleterious mutations in reprogrammed cancer cells.

Our results suggest a specific target for reprogramming in the hypoxia pathway. The expression of Hif2α is cell-type specific and its biological role is distinct from that of Hif1α. While Hif1α is ubiquitously expressed, Hif2α is more prominently detected in vascular endothelial cells during embryonic development and is indeed an upstream regulator of *OCT3/4* (15). Furthermore, in addition to being present in endothelial cells, *HIF2α* mRNA has been detected in kidney fibroblasts, liver hepatocytes, epithelial cells of the intestinal lumen, pancreatic interstitial cells and other interstitial cells (20,21). In this study, the effect of introducing ES-like genes in gastrointestinal cancer cells may have been enhanced by hydroxylation-defective mutation of *HIF2α* and, to a lesser extent, *HIF1α*, suggesting that cell type-specific modifications involving the use of different Hif subunits could be a reliable method of fine-tuning reprogramming efficiency. To the best of our knowledge, this is the first report demonstrating involvement of the Hif family in reprogramming and iPC cell generation.

Acknowledgements

We thank Dr Bert Vogelstein (Johns Hopkins University, Baltimore, MD) for providing *TP53*-deficient cell lines. This work was partly supported by a grant from the Core Research for Evolutional Science and Technology (CREST) (H.I., M.M.), a Grant-in-Aid for Scientific Research on Priority Areas (M.M.), a Grant-in-Aid for Scientific Research from the Ministry of Education, Culture, Sports, Science and Technology (H.I., M.M.), a Grant-in-Aid for the 3rd Comprehensive 10-year Strategy for Cancer Control Ministry of Health, Labour and Welfare (H.I., M.M.), a grant from the Tokyo Biochemical Research Foundation (M.M.) and a grant from the Princess Takamatsu Cancer Research Fund, Japan (H.I.).

References

1. Tenen DG: Disruption of differentiation in human cancer: AML shows the way. Nat Rev Cancer 3: 89-101, 2003.
2. Chen J, Odenike O and Rowley JD: Leukaemogenesis: more than mutant genes. Nat Rev Cancer 10: 23-36, 2010.
3. Markowitz SD and Bertagnolli MM: Molecular origins of cancer: Molecular basis of colorectal cancer. N Engl J Med 361: 2449-2460, 2009.
4. Jones PA and Baylin SB: The fundamental role of epigenetic events in cancer. Nat Rev Genet 3: 415-428, 2002.
5. Piekarz RL and Bates SE: Epigenetic modifiers: basic understanding and clinical development. Clin Cancer Res 15: 3918-3926, 2009.
6. Takahashi K and Yamanaka S: Induction of pluripotent stem cells from mouse embryonic and adult fibroblast cultures by defined factors. Cell 126: 663-676, 2006.
7. Yamanaka S: Elite and stochastic models for induced pluripotent stem cell generation. Nature 460: 49-52, 2009.

8. Miyoshi N, Ishii H, Nagai K, *et al*: Defined factors induce reprogramming of gastrointestinal cancer cells. Proc Natl Acad Sci USA 107: 40-45, 2010.
9. Gil J and Peters G: Regulation of the INK4b-ARF-INK4a tumour suppressor locus: all for one or one for all. Nat Rev Mol Cell Biol 7: 667-677 2006.
10. Zhao Y, Yin X, Qin H, *et al*: Two supporting factors greatly improve the efficiency of human iPSC generation. Cell Stem Cell 3: 475-479, 2008.
11. Kawamura T, Suzuki J, Wang YV, *et al*: Linking the p53 tumour suppressor pathway to somatic cell reprogramming. Nature 460: 1140-1144, 2009.
12. Hong H, Takahashi K, Ichisaka T, *et al*: Suppression of induced pluripotent stem cell generation by the p53-p21 pathway. Nature 460: 1132-1135, 2009.
13. Yoshida Y, Takahashi K, Okita K, Ichisaka T and Yamanaka S: Hypoxia enhances the generation of induced pluripotent stem cells. Cell Stem Cell 5: 237-241, 2009.
14. Yeung SJ, Pan J and Lee MH: Roles of p53, MYC and HIF-1 in regulating glycolysis - the seventh hallmark of cancer. Cell Mol Life Sci 65: 3981-3999, 2008.
15. Poon E, Harris AL and Ashcroft M: Targeting the hypoxia-inducible factor (HIF) pathway in cancer. Expert Rev Mol Med 11: e26, 2009.
16. Ben-Porath I, Thomson MW, Carey VJ, Ge R, Bell GW, Regev A and Weinberg RA: An embryonic stem cell-like gene expression signature in poorly differentiated aggressive human tumors. Nat Genet 40: 499-507, 2008.
17. Takahashi K, Tanabe K, Ohnuki M, Narita M, Ichisaka T, Tomoda K and Yamanaka S: Induction of pluripotent stem cells from adult human fibroblasts by defined factors. Cell 131: 861-872, 2007.
18. Teodoro JG, Evans SK and Green MR: Inhibition of tumor angiogenesis by p53: a new role for the guardian of the genome. J Mol Med 85: 1175-1186, 2007.
19. Nagai K, Ishii H, Miyoshi N, *et al*: Long-term culture following ES-like gene-induced reprogramming elicits an aggressive phenotype in mutated cholangiocellular carcinoma cells. Biochem Biophysic Res Commun 395: 258-263, 2010.
20. Rosenberger C, Mandriota S, Jürgensen JS, *et al*: Expression of hypoxia-inducible factor-1alpha and -2alpha in hypoxic and ischemic rat kidneys. J Am Soc Nephrol 13: 1721-1732, 2002.
21. Wiesener MS, Jürgensen, JS, Rosenberger C, *et al*: Widespread hypoxia-inducible expression of HIF-2alpha in distinct cell populations of different organs. FASEB J 17: 271-273, 2003.

Ann Surg Oncol (2012) 19:2853–2858
DOI 10.1245/s10434-012-2278-6

Annals of
SURGICAL ONCOLOGY
OFFICIAL JOURNAL OF THE SOCIETY OF SURGICAL ONCOLOGY

ORIGINAL ARTICLE – COLORECTAL CANCER

Increased Risk for CRC in Diabetic Patients with the Nonrisk Allele of SNPs at 8q24

Shinya Ishimaru, MD, PhD[1,2], Koshi Mimori, MD, PhD[1], Ken Yamamoto, MD, PhD[3], Hiroshi Inoue, MD, PhD[1], Seiya Imoto, PhD[4], Shuichi Kawano, PhD[4], Rui Yamaguchi, PhD[4], Tetsuya Sato, PhD[5], Hiroyuki Toh, MD, PhD[5], Hisae Iinuma, PhD[6], Toyoki Maeda, MD, PhD[1], Hideshi Ishii, MD, PhD[1], Sadao Suzuki, PhD[7], Shinkan Tokudome, PhD[7], Masahiko Watanabe, MD, PhD[8], Jun-ichi Tanaka, MD, PhD[9], Shin-ei Kudo, MD, PhD[9], Ken-ichi Sugihara, MD, PhD[2], Kazuo Hase, MD, PhD[10], Hidetaka Mochizuki, MD, PhD[10], Masato Kusunoki, MD, PhD[11], Kazutaka Yamada, MD, PhD[12], Yasuhiro Shimada, MD, PhD[13], Yoshihiro Moriya, MD, PhD[13], Graham F. Barnard, MD, PhD[14], Satoru Miyano, PhD[4], and Masaki Mori, MD, PhD[15]

[1]Department of Surgery, Kyushu University Beppu Hospital, Beppu, Japan; [2]Department of Surgery, Tokyo Medical and Dental University, Tokyo, Japan; [3]Department of Molecular and Cellular Biology, Kyushu University, Fukuoka, Japan; [4]Laboratory of DNA Information Analysis, Human Genome Center Institute of Medical Science, University of Tokyo, Tokyo, Japan; [5]Division of Molecular Design, Kyushu University, Fukuoka, Japan; [6]Department of Surgery, Teikyo University, Tokyo, Japan; [7]Department of the Public Health, Nagoya City University, Nagoya, Japan; [8]Department of Surgery, Kitazato University, Sagamihara, Japan; [9]Digestive Disease Center, Northern Yokohama Hospital, Showa University, Yokohama, Japan; [10]Department of Surgery, National Defense University, Tokorozawa, Japan; [11]Department of Surgery, Mie University, Tsu, Japan; [12]Department of Surgery, Takano Hospital, Kumamoto, Japan; [13]Department of Surgery and Digestive Tract Medicine, National Cancer Center, Tokyo, Japan; [14]Department of Medicine, University of Massachusetts Medical School, Worcester, MA; [15]Department of Gastroenterological Surgery, Osaka University, Osaka, Japan

ABSTRACT

Background. Colorectal cancer (CRC) oncogenesis was considered to be determined by interactions between genetic and environmental factors. Specific interacting factors that influence CRC morbidity have yet to be fully investigated.

Methods. A multi-institutional collaborative study with 1511 CRC patients and 2098 control subjects was used to compare the odds ratios for the occurrence of polymorphisms at 11 known single nucleotide polymorphisms (SNPs). TaqMan PCR and questionnaires were used to evaluate the effects of environmental exposures.

Results. Variants of rs6983267 on 8q24 were the most significant markers of risk for CRC (odds ratio 1.16, 95% confidence interval 1.06–1.27, $P = 0.0015$). Non-insulin-dependent diabetes mellitus (DM), a higher body mass index at age 20, and meat consumption were environmental risk factors, whereas a tuna-rich diet and vitamin intake were protective factors. The cohort of rs6983267 SNP major (T) allele at 8q24 and DM had a 1.66-fold higher risk ratio than the cohort of major allele patients without DM.

Conclusions. We confirmed that interactions between the genetic background and environmental factors are associated with increased risk for CRC. There is a robust risk of the minor G allele at the 8q24 rs6983267 SNP; however, a major T allele SNP could more clearly reveal a correlation with CRC specifically when DM is present.

Shinya Ishimaru, Koshi Mimori and Ken Yamamoto contributed equally to this work.

Electronic supplementary material The online version of this article (doi:10.1245/s10434-012-2278-6) contains supplementary material, which is available to authorized users.

First Received: 27 May 2011;
Published Online: 21 March 2012

M. Mori, MD, PhD
e-mail: mmori@gesurg.med.osaka-u.ac.jp

The morbidity and mortality of colorectal cancer (CRC) have been increasing in Japan since 1955. The identification of factors regulating the development and progression

of CRC contributes to improvement of preventive measures and therapeutic outcomes. Three elements are considered to be important in CRC development: host genetic factors (e.g., a single nucleotide polymorphism, or SNP, located within or near a relevant gene); environmental factors that directly affect epithelial cells through cytotoxic effects or genetic damage; and interactions between these genetic and environmental factors.

A number of SNPs have been associated with the onset of CRC. In a genome-wide association study, Tomlinson et al. examined 550,000 SNPs in 930 cases of familial CRC and identified rs6983267 at 8q24 [odds ratio (OR) 1.18, $P = 1.41 \times 10^{-8}$] and 9q24 (OR 1.14, $P = 1.32 \times 10^{-5}$).[1] Other locations, such as 15q13, 18q21, 11q23, 14q22, 16q22, 19q13, and 20p12, have been implicated.[2–5]

Multiple factors are thought to affect the colorectal epithelium during cancer development because the ORs of associated SNPs, including 8q24, for CRC, are less than 2.0. At most, carrying all six possible risk alleles at 8q24 yielded an OR of 2.6 [95% confidence interval (CI) 1.75–3.89] for CRC.[3] Thus, definitive conclusions based only on expression profile data from CRC cells are unlikely; however, the profiles could provide insight into the association between the SNP at 8q24, the incidence of CRC, and the influence of epidemiologic and environmental factors. Among environmental factors affecting CRC oncogenesis, we have specifically focused on diabetes mellitus (DM) because it has been discussed recently in previous studies. Giovannucci et al. clearly demonstrated that diabetes (primarily type 2) is associated with an increased risk of some cancers, including cancer of the colon and rectum, and explained the mechanism of association between DM and CRC with intriguing genes, such as Insulin/Insulin-Like Growth Factor Axis.[6] Previous study found that men with type 2 diabetes were up to 24% more likely to eventually get colon cancer than men without diabetes. Men who used insulin to control their diabetes faced a 36% greater risk of developing colon cancer than men without diabetes.[7]

In the current study, we demonstrate a significant association between a history of DM and the most highly associated SNP, rs6983267, at 8q24, and discuss the relationship.

MATERIALS AND METHODS

Extraction of Genomic DNA and PCR Amplification of Markers

Genomic DNA was extracted from peripheral blood samples from 1511 cases of CRC test subjects and 2098 control subjects by means of conventional methodologies, then quantified with PicoGreen (Invitrogen). The TaqMan probes and primers for rs6983267 and rs10808556 were purchased from Applied Biosystems (assay ID C_29086771_20 and C_31093430_10, respectively). In addition, rs4779584, rs4464148, rs4939827, rs12953717, rs3802842, rs4444235, rs9929218, rs10411210, and rs961253 (chr20:6404031–6404531) were genotyped with the same assay system (Table 1). Genotyping was performed with the ABI 7900HT Sequence Detection System and SDS 2.0 software (Applied Biosystems, Carlsbad, CA).

Evaluation of SNP Markers at 8q24

We evaluated the correlation between the morbidity rate of CRC and SNP rs6983267 at the 8q24 locus. We estimated the risks associated with each SNP by allele and heterozygous and homozygous ORs by an unconditional logistic regression, and calculated the associated 95% CIs in each case. The ethical committee of each institute approved this project.

TABLE 1 Diverse ORs of established SNPs for Japanese CRC cases

Gene or locus	Chromosome	SNP	Minor allele frequency (control)	*P* value for allele test	Effect size, OR (95% CI)
POU5F1P1, DQ515897, MYC	8q24	rs6983267	0.35	0.0016	1.16 (1.06–1.27)
POU5F1P1, DQ515897, MYC		rs10808556	0.34	0.0048	1.14 (1.04–1.25)
SCG5, GREM1, FMN1	15q13	rs4779584	0.17	0.079	ND
SMAD7	18q21	rs4464148	0.04	0.092	ND
		rs4939827	0.21	0.12	ND
		rs12953717	0.19	0.080	ND
LOC120376, FLJ45803, c11orf53, POU2AF1	11q23	rs3802842	0.34	0.085	ND
BMP4	14q22	rs4444235	0.41	0.092	ND
CDH1	16q22	rs9929218	0.18	0.16	ND
RHPN2	19q13	rs10411210	0.16	0.012	1.17 (1.03–1.32)
BMP2	20p12	rs961253	0.12	0.39	ND

Environmental and Epidemiologic Studies and Gene–Environmental Interactions

Detailed information in regard to demographic characteristics was collected via a standardized questionnaire. The information included the following demographic characteristics: height, weight, smoking and drinking habits, activity, sleeping, stress, dietary habits, medical history, present illnesses, drugs, medications and vitamins, body condition, familial diseases, and female-specific diseases. All control subjects had total colon fiber optic examinations to confirm the absence of malignant lesions in the colon and/or the rectum. ORs and 95% CIs were calculated by unconditional logistic regression models, adjusted for sex, age (5-year categories), and study area (Honshu and Kyushu).

For evaluation of genetic and environmental factors, the rs6983267 genotype and lifestyle data were used to evaluate related genetic and environmental factors. Subjects with DM were placed in the environmental risk group, and those with the GG genotype of rs6983267 were designated as a genetic risk group. Subjects with no environmental risk and no genetic risk (TT or GT allele) were treated as the reference group. P values for interaction were based on likelihood ratio tests, comparing models with and without interaction terms. Statistical analyses were performed by SAS software, version 9.1 (SAS, Cary, NC). A two-tailed P value of less than 0.05 was used to indicate statistical significance.

Statistical Analysis

The magnitude of carcinogenicity for established CRC SNPs was determined by a case–control study, and the related epidemiologic and environmental factors were defined through self-administered questionnaires. A significant internal association was found between rs6983267, a SNP at 8q24, and a history of DM.

RESULTS

Significant Correlation between CRC Morbidity and rs6983267

Three SNPs—rs6983267, rs10808556 at 8q24, and rs10411210 at 19q13—were significantly correlated with the incidence of CRC (Table 1).[3,5,8,9] Table 2 indicates that allelic testing determined that variant rs6983267 at 8q24 was significantly associated with CRC (OR 1.16, 95% CI 1.06–1.27, $P = 0.0015$).[8,10,11] Another variant, rs10808556, also had a significant correlation (OR 1.14, 95% CI 1.04–1.25). However, rs6983267 in 8q24 showed the strongest association among the three SNPs. As such, the 8q24 locus, with its association between the G allele and CRC risk, is the focus of further investigations here on the mechanism of CRC development.[12]

Epidemiologic and Environmental Risk Factors for CRC

As we indicate in the Supplementary Tables, there were numerous number of CRC oncogenesis–associated epidemiologic factors. The average age was significantly higher in 1511 cases (63.72) than 2098 control subjects (60.80) ($P < 0.0001$, Student's t-test, Supplementary Table 1). Weight at present was heavier in control subjects (59.35 kg) than in cases (58.53 kg) ($P = 0.0298$). For smoking, the total smoking period was much longer in cases (30.51 years) than in control subjects (28.75 years), which was statistically significant ($P = 0.0082$). In those who drank alcohol, the period since stopping drinking was shorter in cases (5.21 years) than in control subjects (9.60 years), which was statistically significant ($P < 0.0001$). For the sort of alcohol drunk, Japanese sake, distilled spirit, whiskey, and wine were statistically significantly associated with a higher risk for CRC.

In Supplementary Table 3, we present the frequency of food diversely. We discovered that patients had significantly

TABLE 2 OR of SNPs (rs6983267 and rs10808556) at 8q24 loci for CRC

SNP	Location	Test	Frequency		P	OR	95% CI	Hardy–Weinberg test
			Case	Control				
rs10808556	128482329	Allelic test	0.368	0.338	0.005	1.14	1.04–1.25	0.86
		Dominant model	0.601	0.56	0.009	1.18	1.04–1.34	
		Recessive model	0.134	0.115	0.062	1.19	0.99–1.44	
rs6983267	128482487	Allelic test	0.384	0.35	0.002	1.16	1.06–1.27	0.93
		Dominant model	0.616	0.579	0.016	1.17	1.03–1.33	
		Recessive model	0.153	0.122	0.004	1.3	1.09–1.55	